

Cite as: AIP Advances 12, 065012 (2022); https://doi.org/10.1063/5.0096893 Submitted: 27 April 2022 • Accepted: 20 May 2022 • Published Online: 08 June 2022

Daniel Sadowsky

COLLECTIONS



This paper was selected as an Editor's Pick









ARTICLES YOU MAY BE INTERESTED IN

Investigation of a nanostructured GaP/MoS₂ p-n heterojunction photodiode AIP Advances 12, 065004 (2022); https://doi.org/10.1063/5.0089842

First-principles study of electronic and optical properties of small edge-functionalized penta-graphene quantum dots

AIP Advances 12, 065008 (2022); https://doi.org/10.1063/5.0091475

Effects of current rate on electrically exploding aluminum wires in argon gas AIP Advances 12, 065210 (2022); https://doi.org/10.1063/5.0095749





Universal anharmonic potential energy surfaces

Cite as: AIP Advances 12, 065012 (2022); doi: 10.1063/5.0096893

Submitted: 27 April 2022 • Accepted: 20 May 2022 •

Published Online: 8 June 2022







Daniel Sadowsky^{a)}



AFFILIATIONS

Division of Physical and Computational Sciences, University of Pittsburgh at Bradford, 300 Campus Drive, Bradford, Pennsylvania 16701, USA

a) Author to whom correspondence should be addressed: sadowsky@pitt.edu

ABSTRACT

An approach to generate anharmonic potential energy surfaces for both linear and bent XY_2 -type molecules from their equilibrium geometries, Hessians, and total atomization energies alone is presented. Two key features of the potential energy surfaces are that (a) they reproduce the harmonic behavior around the equilibrium geometries exactly and (b) they have the correct limiting behavior with respect to total bond dissociation. The potentials are constructed from two diatomic potentials, for which both the Morse or Varshni potentials are tested, and a triatomic potential, for which modified forms of the Anderson-n potential are tested. Potential energy surfaces for several linear and bent molecules are constructed from ab initio data, and the third-order derivatives of these surfaces at their equilibrium geometries are compared to the results of finite difference computations. For bent molecules, the vibrational spectra predicted by vibrational configuration interaction calculations on these surfaces are compared to experiment. A modified version of the Anderson-n potential, in combination with the Varshni potential, is demonstrated to predict vibrational frequencies associated with bond angle bending an average of 20 cm⁻¹ below the harmonic oscillator approximation and with a fourfold reduction in the root-mean-square deviation from experiment compared to the harmonic oscillator approximation.

© 2022 Author(s). All article content, except where otherwise noted, is licensed under a Creative Commons Attribution (CC BY) license (http://creativecommons.org/licenses/by/4.0/). https://doi.org/10.1063/5.0096893

I. THEORY

Computational electronic structure methods have come of age; for example, the computation of highly accurate equilibrium geometries, Hessians, and relative energies is now routine for moderately sized polyatomic molecules. Accurate computational vibrational structure methods, such as vibrational configuration interaction (VCI)¹⁻⁴ and vibrational coupled-cluster,⁵⁻⁷ have also been available for many years; however, most routine thermochemistry calculations continue to make use of the harmonic oscillator (HO) approximation for the computation of vibrational partition functions. As the availability of computational resources continues to dramatically increase, and the use of higher accuracy electronic structure methods has become more commonplace, the relative contribution of the HO approximation to the total error of thermochemical calculations has increased to the point where it is not uncommon for the HO approximation to be a major source of error in routine thermochemical calculations. 8-10 A major reason for the persistence of the

HO approximation in computational thermochemistry is the high computational intensity of the fourth- and/or sixth-order derivative tensors necessary to construct an anharmonic potential energy surface from a Taylor series expansion around an equilibrium geometry.4 We, therefore, consider an alternative to this Taylor series expansion: estimation of the anharmonic behavior around an equilibrium geometry by constraining the potential energy surface to have qualitatively and/or quantitatively correct behavior upon the dissociation of one or more bonds. In doing this, we take inspiration from the Morse potential¹¹ [Eq. (5)], a three-parameter bonding potential that does just that for diatomics: it requires only the bond length, harmonic constant, and bond dissociation energy as parameters. The Morse potential has been widely used to model the potential energy curves of covalent, ionic, and metallic bonds, and even van der Waals dimers, a success which it owes no doubt to its simplicity and correct limiting behavior. Without the need for any explicit numerical computation of higher-order derivatives, the

Morse potential can be used to obtain a reasonably good estimate for the anharmonic behavior of a diverse range of diatomic interactions. This work supposes that similarly universal anharmonic potentials can be derived for polyatomic molecules as well. A general approach is proposed and applied to the cases of linear and bent XY_2 -type molecules.

A. The general approach

The form of the potential, U, of a molecule in the general approach that we propose is a sum of independent "local" potentials. These could include diatomic bonding potentials (U_{abc}), triatomic bond angle bending potentials (U_{abc}), and tetratomic dihedral or improper torsional potentials (U_{abcd}),

$$U = \sum_{abc}^{n_{bonds}} U_{ab} + \sum_{abc}^{n_{bends}} U_{abc} + \sum_{abc}^{n_{torsions}} U_{abcd}. \tag{1}$$

However, attempting to fit such a flexible and complex potential to a single equilibrium geometry and Hessian could result in an illposed problem. One strategy to avoid this would be to introduce some additional constraints on the nature of the constituent local potentials, which enforce a strict separability:

- Each local potential must have a value of zero at the equilibrium geometry of the molecule.
- Each local potential must have critical point at the equilibrium geometry of the molecule (i.e., the first derivatives with respect to the movement of any atom must be zero).
- Each local potential must have the harmonic behavior (i.e., second derivatives with respect to the movement of any atom or pair of atoms) at the equilibrium geometry of the molecule, which is assigned to it (e.g., a harmonic bond stretch), and no additional harmonic behavior.
- Each bonding potential, U_{ab}, has a bond dissociation energy assigned to it, which may be either estimated or explicitly computed. The potential must have this value as its limit with respect to the dissociation of bond AB.
- Each triatomic potential, U_{abc}, must have a limit of zero with respect to the dissociation of bond AB, bond BC, and both bonds.
- Each tetratomic potential, U_{abcd}, must similarly have a limit of zero with respect to the dissociation of any bond between atoms A, B, C, and D, and to any combination of such bonds.

B. Symmetric molecules

One challenge in extending the Morse approach to polyatomic molecules is that there can be multiple bonds in a molecule with unique bond dissociation energies (E_{BD}). A result of this is that several quantities, which cannot be derived from the equilibrium geometry of a molecule, must be known in order to correctly constrain the limiting behavior of the potential energy surface. Explicit computation of bond dissociation values can require separate electronic structure calculations of several radical species, which does not lend itself to routine implementation. In some cases, it may be judged that quantitatively accurate behavior in the limit of single bond dissociation (that is, dissociation to the explicitly computed bond dissociation energy) may be worth this effort. However, the motivation for the approach proposed here is the need to estimate

the anharmonic behavior of a molecule around geometry with minimal additional computation. Several schemes have been proposed to estimate bond dissociation energies from electronic structure calculations, ^{12–16} and these may suffice in many situations.

However, while the limits with respect to the dissociation of a single bond may require estimation, one limit, which is rather simple to determine from explicit computation, is the limit of the energy with respect to the dissociation of all bonds or the total atomization energy (E_{TA}). Although most electronic structure programs return electronic energies rather than total atomization energy values, the total atomization energy of a molecule is easily derived from its electronic energy, and the sum of the electronic energies of each atom is computed at the same level theory. For symmetric molecules with only one unique bond, the total atomization energy could conceivably be used as the *only* piece of information, which constrains the potential energy surface other than the equilibrium geometry and Hessian; for example, each bond dissociation energy could be estimated from the total atomization energy and the number of bonds (n_{bonds}),

$$E_{BD} = \frac{E_{TA}}{n_{bonds}}. (2)$$

This allows for the construction of an anharmonic potential energy surface with essentially the same amount of computational complexity as the computation of the equilibrium geometry and Hessian, which are also necessary for the construction of a harmonic potential energy surface. The resulting anharmonic surface, however, has the correct behavior in the limit of the dissociation of all bonds and a reasonable estimate for the behavior in the limit of the dissociation of a single bond. Although a general method for the construction of anharmonic potential energy surfaces for polyatomic molecules necessarily involves either the estimation or explicit computation of bond dissociation energies, the approximation in Eq. (2) provides a framework to test and evaluate general methods for polyatomic potentials independently of the development and evaluation of estimation methods for bond dissociation energies.

C. XY2-type molecules

In the case of a symmetric triatomic molecule, the general form in Eq. (1) yields only two (identical) bonding potentials and a single triatomic potential,

$$U(r_1, r_2, \theta_3) = \sum_{i=1}^{2} U_i(r_i) + U_{12}(r_1, r_2, \theta_3).$$
 (3)

Following Eq. (2), each bonding potential will dissociate to half the value of the explicitly computed total atomization energy. For linear XY_2 -type molecules, we assume a single well on the potential energy surface at $\theta=\pi$; for bent XY_2 -type molecules, we assume two wells at $\theta=\theta_e$ and $\theta=-\theta_e$ and a first-order saddle point at $\theta=\pi$. If the Hessian is computed in the internal coordinates (r_1,r_2,θ_3) , the Hessian of linear molecules contains four non-zero terms: the identical bond stretch terms k_{11} and k_{22} , which are assigned to the bonding potentials, the bond–bond cross-term k_{12} , which is assigned to the triatomic potential, and the bending term k_{33} , which is also assigned to the triatomic potential. The Hessian of bent molecules contains

two additional non-zero terms, k_{13} and k_{23} , which are identical and are assigned to the triatomic potential. Therefore, in total, we have three unique non-zero data points to fit the bonding potentials for both linear and bent XY_2 -type molecules: k_{11} , E_{TA} , and the equilibrium bond length, r_e . For linear molecules, we have two data points to fit the triatomic potentials, k_{12} and k_{33} . Finally, we have five data points to fit the triatomic potentials for bent molecules: k_{12} , k_{33} , k_{13} , k_{23} , and the equilibrium bond angle, θ_e .

D. Bonding potentials

1. Harmonic potential

The HO approximation, as applied to bonding potentials, is a two-parameter potential with incorrect limiting behavior, but we will consider it as a reference,

$$U(r) = \frac{1}{2}k_e(r - r_e)^2.$$
 (4)

The HO approximation strongly overestimates vibrational frequencies associated with bond stretching.

2. Morse potential

The Morse potential is a three-parameter potential first described in 1929.¹¹ It is widely used in the spectroscopy of diatomic molecules, although it has been partially displaced in popularity by more accurate potentials with additional parameters. However, it is now finding increasing use in molecular modeling^{17–19} due to its conceptual and computational simplicity,

$$U(r) = D_e \left(1 - e^{-\alpha(r - r_e)} \right)^2.$$
 (5)

3. Varshni potential

While the Morse potential is perhaps the simplest three-parameter diatomic potential, it is not the only functional form that meets the same constraints, and not necessarily the form that best models covalent bonding. Generally, the Morse potential tends to be too soft, slightly overestimating the anharmonicity of bond stretches. Several other three-parameter bonding potentials have been suggested, of which the Varshni²⁰ potential has been shown to be one of the more reliably accurate, ²¹

$$U(r) = D_e \left(1 - \frac{r_e}{r} e^{-\beta (r^2 - r_e^2)} \right)^2.$$
 (6)

E. Triatomic potentials

1. Harmonic potential

The HO approximation, as applied to the parts of the Hessian assigned to the triatomic potential, also does not have the correct limiting behavior but is considered as a reference,

$$U_{12}(r_1, r_2, \theta_3) = \frac{1}{2} k_{33} (\theta_3 - \theta_e)^2 + k_{12} (r_1 - r_e) (r_2 - r_e)$$

$$+ k_{13} (r_1 - r_e) (\theta_3 - \theta_e)$$

$$+ k_{23} (r_2 - r_e) (\theta_3 - \theta_e).$$
(7)

Bending vibrational modes are generally less anharmonic than bond stretching modes. One source of anharmonicity is that bond angle bends tend to have positive fourth derivatives, which have the effect of stiffening bending potentials. However, the angular dependence of molecular potentials vanishes as either one or both of the bonds that form the angle dissociate, which has the effect of softening bending potentials. This second phenomenon has a larger effect on vibrational frequencies and is enhanced by the anharmonicity of bond stretches, which causes the average bond length of the ground state of molecules to be longer than the equilibrium bond lengths where the angular dependence of the molecular potential is softer. Therefore, the HO approximation tends to slightly overestimate vibrational frequencies associated with bond angle bending.

2. Anderson-n potential

The Anderson-n potential^{22,23} for linear triatomics describes bond angle bending in terms of the distance between the terminal atoms, r_{12} ,

$$r_{12} = \sqrt{r_1^2 + r_2^2 - 2r_1r_2 \cos(\theta_3)}.$$
 (8)

The model contains two optimized parameters and a fixed parameter, which has a recommended value of n = 4,

$$U_A^{(n)} = \frac{\alpha}{r_{12}^n} + \frac{\beta}{(r_1 + r_2)^n}.$$
 (9)

This potential can be used to represent the harmonic bending term and the harmonic bond–bond cross-term and has the correct limiting behavior (it vanishes with the dissociation of either one or both bonds). The description of the bond angle bending in terms of an inverse power r_{12} , rather than the angle, corrects for both problems with the harmonic treatment of the triatomic potential described above. The second term in Eq. (9) reproduces the harmonic behavior of the bond–bond cross-term. The advantage of the model in Eq. (9) is that it is probably the simplest expression, both conceptually and computationally, for describing the harmonic behavior of the triatomic potential while also having the correct limiting behavior and qualitatively correct anharmonicity. It is simple enough, in fact, that analytical expressions for the parameters, α and β , can be derived in terms of the geometry and Hessian data, for example, if

$$\alpha_A^{(4)} = 16k_{33}r_e^4,\tag{10}$$

$$\beta_A^{(4)} = \alpha - \frac{16}{5} k_{12} r_e^6. \tag{11}$$

3. Modified Anderson-n (mA-n) potential

However, the Anderson-*n* potential has a non-zero value and non-zero first and second derivatives at the equilibrium geometry. While the non-zero value of the potential could be easily fixed by an intercept term, the non-zero value of the derivatives makes the potential incompatible with the method outlined in Sec. I A. Moreover, a triatomic potential with non-zero derivatives at the equilibrium geometry ensures that the diatomic potential must also

have non-zero derivatives at the equilibrium geometry, and thus a minimum at bond length other than the equilibrium bond length. While a diatomic fragment formed by the dissociation of a terminal atom from a triatomic molecule should not have the same equilibrium bond length as the triatomic equilibrium bond length, the diatomic fragment bond lengths predicted incidentally by the fitting of the Anderson-n potential to an equilibrium geometry can be highly unphysical. A solution to this problem is to modify the Anderson-n potential to include five additional parameters,

$$U_{mA}^{(n)} = \frac{\alpha}{r_{12}^n} + \frac{\beta_0}{r_1 r_2} + \frac{\beta_1}{r_1^2 r_2} + \frac{\beta_2}{r_1 r_2^2} + \frac{\beta_3}{r_1^3 r_2} + \frac{\beta_4}{r_1^2 r_2^2} + \frac{\beta_5}{r_1 r_2^3}.$$
 (12)

Fitting such potential requires five additional constraints; in this case, we demand that the potential and its first and second derivatives with respect to r_1 and r_2 are zero at the equilibrium geometry. As a consequence of this, the modified potential in Eq. (12) meets all of the requirements for separable local potentials proposed in Sec. I A. One advantage of this approach is the stability of the method across the entire chemical space of linear triatomic molecules. However, the modified potential also creates a flexible framework in which either the constraints of Sec. I A can be applied, or if the need for greater accuracy is judged to be worth the additional effort, constraints derived from the explicit computation of the bond dissociation energy as well as the bond length and harmonic constant of the diatomic fragment formed by single bond dissociation can be applied.

4. Extensions to bent XY 2-type molecules

Extending such a potential to bent XY_2 -type molecules requires three additional parameters. We propose an additional term, which is an inverse power of the distance between a terminal atom and a dummy point, r_{12} ,

$$U_{bent}^{(n)} = U_{linear}^{(n)} + \frac{\gamma_0 + \gamma_1 r_1 + \gamma_2 r_2}{r_{12}^n}.$$
 (13)

The dummy point could be placed in the plane of the molecule, a distance from the central atom equal to the bond distance to the other terminal atom, directly opposite the direction that bisects the bond angle (see Fig. 1). Such a dummy point simulates the effect of a single lone pair of electrons and is subsequently referred to as the "planar" model. In this model, the distance between each terminal atom and its dummy atom is identical,

$$r_{12'} = \sqrt{r_1^2 + r_2^2 - 2r_1r_2 \cos\left(\pi - \frac{\theta_3}{2}\right)}.$$
 (14)

An alternative definition of $r_{12'}$ would be a similar dummy point, the same distance from the central atom and at the same angle in the plane, but rotated out of the plane of the molecule at an angle equal to half of the bond angle, θ_3 . Such dummy points simulate the

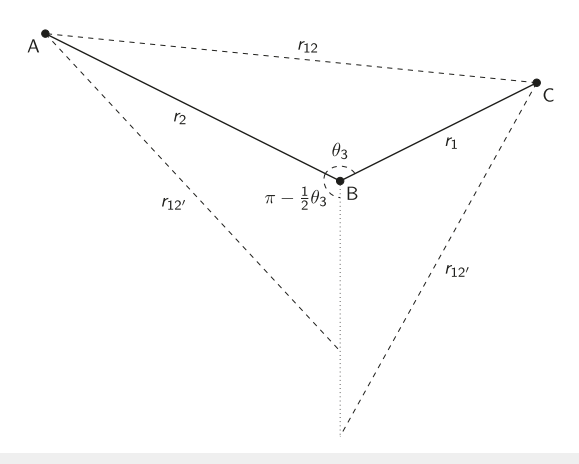


FIG. 1. A bent XY_2 -type molecule with atoms A, B, and C with the bond lengths $(r_1$ and $r_2)$, the distance between the terminal atoms (r_{12}) , and the distances between the terminal atoms and their in-plane dummy points (r_{12}) displayed.

effect of two lone pairs of electrons and are subsequently referred to as the "out-of-plane" model. In this model, the distance between each terminal atom and each of its dummy atoms is identical,

$$r_{12'} = \sqrt{\left(r_1^2 + r_2^2\right)\sin^2\left(\frac{\theta_3}{2}\right) + \left(r_1 + r_2\right)^2\cos^2\left(\frac{\theta_3}{2}\right)}.$$
 (15)

II. COMPUTATIONAL DATA SET

Numerical derivatives are computed around the equilibrium geometry of 10 linear molecules and 15 bent molecules (see Table I). A seventh-order finite difference stencil and a finite difference parameter of 5 pm are used.

III. EXPERIMENTAL DATA

A subset of the bent molecules under consideration had critically evaluated experimental data for fundamental vibration frequencies. $^{24-27}$ All available data that were critically evaluated with estimated uncertainties less than 5 \mbox{cm}^{-1} are included, and these values are presented in Table II.

TABLE I. The sets of linear and bent XY₂-type molecules for which potential energy surfaces are constructed.

	Linear			Bent	
BeH ₂ BeF ₂ BeCl ₂ SiS ₂	MgH ₂ MgF ₂ MgCl ₂	CO ₂ CS ₂ SiO ₂	CH ₂ CF ₂ CCl ₂ OH ₂ OF ₂	O ₃ OCl ₂ SiH ₂ SiF ₂ SiCl ₂	SH ₂ SO ₂ SF ₂ S ₃ SCl ₂

TABLE II. The experimental vibrational frequencies used in all comparisons with computed vibrational frequencies. Unless otherwise noted, the frequencies are for the most abundant isotope of each atom.

	$1a_1$	$2a_1$	$1b_1$	References
OF ₂	461	928	831	24
OH_2	1595	3657	3756	26
O_3	701	1103	1042	25
SH_2	1183	2615	2626	24
SO_2	518	1152	1362	27

IV. METHODS

A. Electronic structure calculations

Unless otherwise noted, all electronic structure calculations are implemented in $PSI4^{28}$ using coupled-cluster through perturbative triples [CCSD(T)] and the aug-cc-pVTZ basis set.^{29–31}

B. Vibrational structure calculations

The analytical derivatives of all model potentials up to sixth-order are computed using SymPy,³² and these derivatives are converted into normal mode coordinates using PyPES.³³ Fundamental vibrational modes are computed for each normal-mode potential energy surface with VCI calculations in PyVCI⁴ using the default settings. The PyPES input files were generated using a Python script, which is freely available.³⁴

V. RESULTS

A. Third-order derivatives of linear triatomic potentials

For linear XY_2 -type molecules, there are three symmetryunique non-zero third derivatives in internal coordinates. The predictions of the bond-stretch third derivative, k_{111} , are affected primarily by the choice of bonding potential, U_{ab} . However, the constraints introduced to ensure the separability of the local potentials ensure that the predictions of the bond-stretch cross-term, k_{112} , and the bond-stretch-angle-bend cross-term, k_{133} , are affected only by the choice of triatomic potential, U_{abc} . The mean signed deviations (MSD) and root-mean-square deviations (RMSD) from explicit finite difference computations of the predictions of these derivatives made by the harmonic oscillator approximation and by the modified Anderson-n method with values of n ranging from 2 to 6 are reported in Table III.

The ability of the methods under consideration to model the anharmonicity of the coupling of bond stretches is probably fundamentally limited by the approximation made in Eq. (2). However, both the modified Anderson-2 and modified Anderson-3 methods predict k_{112} terms with half the RMSD of the harmonic oscillator approximation. Interestingly, the modified Anderson method predicts k_{112} that are too negative, as evidenced by the MSD (while the harmonic oscillator approximation predicts a k_{112} value of zero by definition). The modified Anderson-n potentials make a more substantial correction to the anharmonic coupling of the bond stretches to the bond angle bends, as evidenced by the k_{133} predictions. The

TABLE III. Mean signed deviations (MSDs) and root-mean-square deviations (RMSDs) from explicit finite difference computations of the internal coordinate third-order cross-term derivative predictions, in atomic units, of potentials constructed with various triatomic approximations for ten linear XY₂-type molecules.

Derivative	Triatomic potential	MSD	RMSD
	HO ^a	0.017	0.034
_	mA-2 ^b	-0.006	0.014
k_{112}	mA-3	-0.008	0.015
	mA-4	-0.011	0.019
	mA-5	-0.016	0.027
	mA-6	-0.026	0.040
	НО	0.043	0.059
	mA-2	0.013	0.024
k_{133}	mA-3	-0.002	0.012
	mA-4	-0.017	0.019
	mA-5	-0.032	0.036
	mA-6	-0.047	0.054

^aEquation (7).

modified Anderson-3 potential, in particular, reduces the RMSD of the k_{133} predictions by a factor of 5 in comparison to the HO approximation. The modified Anderson-2 potential slightly underestimates the anharmonicity, predicting k_{133} constants that are too close to zero (as evidenced by the mean signed deviations) and in worse agreement with the finite difference calculations than the modified Anderson-3 potential (as evidenced by the root-mean-square deviations). Likewise, the modified Anderson-4 potential slightly overestimates the anharmonicity, predicting k_{133} constants that are too negative and in worse agreement with the finite difference calculations than the modified Anderson-3 potential.

B. Third-order derivatives of bent triatomic potentials

For bent XY_2 -type molecules, there are six symmetry-unique non-zero third derivatives in internal coordinates. With the exception of the k_{111} term, these derivatives are affected only by the choice of triatomic potential, U_{abc} , and MSD and RMSD from explicit finite difference computation of each of the predictions made by both the planar and out-of-plane modified Anderson methods of these derivatives are reported in Table IV.

The predictions made by all of the modified Anderson-n methods for the k_{112} term are also not particularly good for bent XY_2 molecules, with only marginal improvements over the harmonic oscillator method. However, considerable improvements were made in the third derivative involving the bond angle bend, θ_3 , especially for the planar model. Predictions of the k_{113} and k_{123} terms were best with the planar mA-4 method, with twofold and threefold improvements over the RMSD of the harmonic oscillator approximation, respectively. Predictions of the k_{133} and k_{333} terms were best with the planar mA-5 method, with threefold and fourfold improvements over the RMSD of the harmonic oscillator approximation, respectively. Interestingly, the out-of-plane methods make similar predictions to the planar methods for every third derivative except for the k_{333} term. The out-of-plane method predicts k_{333} terms that

^bEquation (12).

TABLE IV. Mean signed deviations (MSD) and root-mean-square deviations (RMSD) from explicit finite difference computations of the internal coordinate third-order cross-term derivative predictions, in atomic units, of potentials constructed with various triatomic approximations for ten linear XY_2 -type molecules.

Derivative	Triatomic potential	MSD	RMSD	
	HOª	0.029	0.047	
	mA-2 ^b (planar) ^c	0.010	0.041	
	mA-3 (planar)	-0.008	0.042	
	mA-4 (planar)	-0.010	0.044	
	mA-5 (planar)	-0.009	0.046	
	mA-6 (planar)	-0.009	0.050	
k_{112}	mA-2 (oop) ^d	0.010	0.038	
	mA-3 (oop)	-0.007	0.040	
	mA-4 (oop)	-0.011	0.044	
	mA-5 (oop)	-0.014	0.048	
	mA-6 (oop)	-0.017	0.052	
	НО	0.058	0.077	
	mA-2 (planar)	0.037	0.054	
	mA-3 (planar)	0.026	0.042	
	mA-4 (planar)	0.015	0.035	
	mA-5 (planar)	-0.009	0.042	
	mA-6 (planar)	-0.007	0.035	
k_{113}	mA-2 (oop)	0.034	0.049	
•113	mA-3 (oop) 0.023		0.039	
	mA-4 (oop)	0.012	0.033	
	mA-5 (oop)	-0.001	0.032	
	mA-6 (oop)	-0.011	0.036	
	НО	0.046	0.063	
	mA-2 (planar)	0.018	0.032	
	mA-3 (planar)	0.006	0.023	
	mA-4 (planar)	-0.005	0.020	
	mA-5 (planar)	-0.016	0.027	
	mA-6 (planar)	-0.027	0.037	
k_{123}	mA-2 (oop)	0.021	0.035	
	mA-3 (oop)	0.010	0.025	
	mA-4 (oop)	-0.002	0.020	
	mA-5 (oop)	-0.013	0.024	
	mA-6 (oop)	-0.024	0.034	
	НО	0.198	0.243	
	mA-2 (planar)	0.113	0.154	
	mA-3 (planar)	0.065	0.109	
	mA-4 (planar)	0.017	0.074	
	mA-5 (planar)	-0.032	0.070	
	mA-6 (planar)	-0.080	0.100	
k_{133}	mA-2 (oop)	0.099	0.138	
	mA-3 (oop)	0.052	0.096	
	mA-4 (oop)	0.005	0.068	
	mA-5 (oop)	-0.042	0.073	
	mA-6 (oop)	-0.089	0.107	

TABLE IV. (Continued)

Derivative	Triatomic potential	MSD	RMSD
	НО	0.594	0.691
	mA-2 (planar)	0.239	0.338
	mA-3 (planar)	0.147	0.260
	mA-4 (planar)	0.060	0.203
	mA-5 (planar)	-0.022	0.177
	mA-6 (planar)	-0.105	0.193
k_{333}	mA-2 (oop)	-0.050	0.203
	mA-3 (oop)	-0.108	0.214
	mA-4 (oop)	-0.167	0.242
	mA-5 (oop)	-0.225	0.281
	mA-6 (oop)	-0.284	0.327

^aEquation (7).

are too negative for all values of n considered. Both the overly soft bending of the out-of-plane potentials and the agreement of the out-of-plane potentials with the numerically computed third derivatives worsen with higher values of the n parameter.

However, another difference between the planar and out-of-plane models is that while the out-of-plane model correctly predicts a critical point on the potential energy surface at a bond angle of $\theta_3 = \pi$, the planar model has a discontinuity on its potential energy surface. Figures 2 and 3 show cross sections of the bond angle bending coordinate of potential energy surfaces generated with these

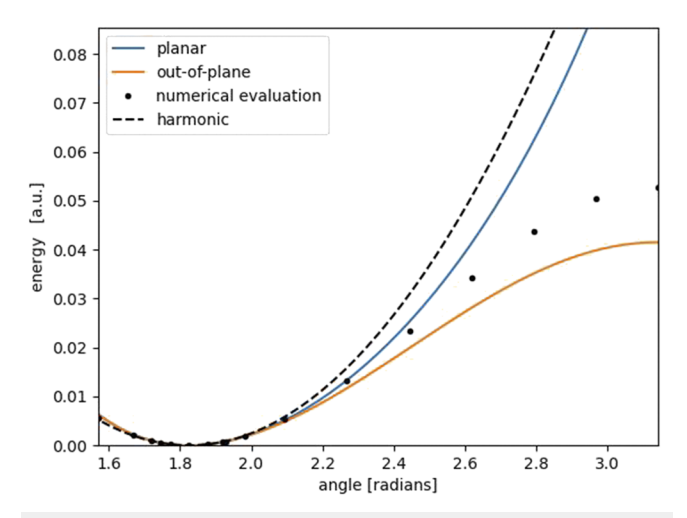


FIG. 2. The potential of an H₂O molecule fit with the mA-5 planar [Eq. (14)] and mA-2 out-of-plane [Eq. (15)] potentials as a function of the bond angle bend, θ_3 , at the equilibrium bond lengths of r_1 and r_2 .

^bEquation (12).

^cEquation (14).

d Equation (15).

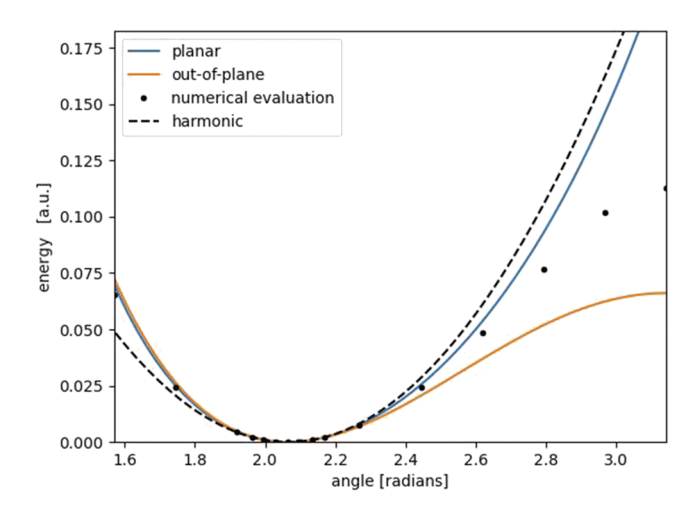


FIG. 3. The potential of an SO₂ molecule fit with the mA-5 planar [Eq. (14)] and mA-2 out-of-plane [Eq. (15)] potentials as a function of the bond angle bend, θ_3 , at the equilibrium bond lengths of r_1 and r_2 .

methods for H_2O and SO_2 , respectively, with both bond lengths constrained to their equilibrium values. The planar and out-of-plane methods that are demonstrated to best predict the third derivative of the bond angle bending coordinate, k_{333} , in Table IV (which are, respectively, n=5 and n=2) are used. For both H_2O and SO_2 , the out-of-plane model underpredicts the linearization barrier height. While the planar model has the wrong qualitative behavior, it is in closer quantitative agreement with the numerical evaluation of the H_2O and SO_2 surfaces than the out-of-plane methods close to equilibrium.

C. Fundamental vibrational frequencies

The MSD and RMSD from the experiment of the vibrational frequency predictions made by VCI calculations on the model potential energy surfaces are reported in Table V. With the harmonic triatomic potential, both the Morse and Varshni diatomic potentials resulted in much greater agreement with the experiment than the harmonic bonding potential. They both reduced the overall RMSD by a factor of 4, but their effect was not limited to the two bond stretch modes. Both the Morse and the Varshni potentials also softened the $1a_1$ bond angle bending modes by over 10 cm⁻¹ and lowered the RMSD of the $1a_1$ modes by a factor of 2. The use of the planar triatomic potential with the Morse and Varshni potential resulted in even better agreement than the harmonic triatomic potential. The $1a_1$ modes softened and had reduced RMSD from the experiment with increasing values of the parameter n. For both the Morse and Varshni potentials, the planar mA-6 potential predicted the $1a_1$ frequencies with the best agreement with the experiment, with an approximately fourfold reduction in the RMSD. The overall agreement with the planar mA-6 potential was better for the Varshni bond potential, as the Morse potential overestimates bond stretch anharmonicity and thus underestimates the bond stretch frequencies. The use of the out-of-plane triatomic potential with both the Morse and Varshni bonding potentials resulted in an overestimation

TABLE V. Mean signed deviations (MSD) and root means signed deviations (RMSD) from the experiment of the fundamental frequency predictions, in cm⁻¹, of potentials constructed with various diatomic and triatomic approximations for five bent XY₂-type molecules (see Table II for experimental data).

		$1a_1$	$1a_1$ mode		nodes
Diatomic potential	Triatomic potential	MSD	RMSD	MSD	RMSD
НО	НО	21.0	29.4	52.6	82.1
	НО	8.1	13.7	-4.4	21.4
	mA-2 (planar)	8.5	14.3	-4.4	21.9
	mA-3 (planar)	4.9	10.3	-10.7	25.4
	mA-4 (planar)	2.5	8.5	-11.1	25.1
	mA-5 (planar)	0.5	7.6	-10.4	23.9
	mA-6 (planar)	-0.9	7.4	-9.0	22.9
Morse	mA-2 (oop)	-7.4	16.8	-11.7	23.1
	mA-3 (oop)	-10.9	20.4	-15.6	26.4
	mA-4 (oop)	-13.6	23.1	-15.7	26.8
	mA-5 (oop)	-15.6	25.0	-15.2	26.7
	mA-6 (oop)	-16.7	25.8	-14.8	26.5
	НО	8.8	14.4	4.2	19.3
	mA-2 (planar)	9.5	15.3	4.2	20.4
	mA-3 (planar)	6.2	11.6	-1.4	18.7
	mA-4 (planar)	4.0	9.5	-1.4	18.5
	mA-5 (planar)	2.3	8.3	-0.7	18.5
	mA-6 (planar)	1.0	7.8	0.1	18.8
Varshni	mA-2 (oop)	-6.4	16.4	-2.7	19.7
	mA-3 (oop)	-9.8	19.7	-6.4	20.2
	mA-4 (oop)	-12.1	22.1	-6.6	21.0
	mA-5 (oop)	-13.9	23.7	-6.2	21.7
	mA-6 (oop)	-14.9	24.3	-5.8	22.2

of bend anharmonicity and an underprediction of the $1a_1$ vibrational frequency, with the agreement with the experiment worsening with increasing values of the parameter n.

As the Varshni potential with the planar mA-5 potential predicts vibrational frequencies with the best overall agreement with the experiment, these predictions are compared with the predictions made from analogous surfaces fitted to MP2 and CCSD calculations instead of CCSD(T) calculations. These predictions are reported in Table VI, along with their corresponding harmonic frequencies and frequencies predicted by a combination of the Varshni potential and the harmonic triatomic potential. As expected, the treatment of electron correlation has a big impact on vibrational frequency predictions, and the overall agreement of the harmonic frequencies with the experiment (and quantified by the RMSD of all modes) improves smoothly with higher levels of electron correlation treatment. Interestingly, the harmonic bending mode has a worse agreement with the experiment with CCSD than it does with MP2, which has a similar agreement to CCSD(T). However, for all three levels of theory, the replacement of the harmonic diatomic potential with the Varshni potential increases the agreement with the experiment, as

TABLE VI. Mean signed deviations (MSD) and root mean signed deviations (RMSD) from the experiment of the fundamental frequency predictions, in cm $^{-1}$, of potentials constructed with various diatomic and triatomic approximations from various levels of electronic structure theory for five bent XY_2 -type molecules (see Table II for experimental data).

			$1a_1$ mode		All modes	
Electronic structure theory	Diatomic Triatomic potential potential	MSD	RMSD	MSD	RMSD	
	НО	НО	19.6	30.4	136.3	325.0
MP2/aTZ	Varshni	НО	5.6	19.4	73.9	286.6
	Varshni	mA-6 (planar)	0.3	18.9	74.9	285.8
	НО	НО	46.8	50.5	112.1	132.7
CCSD/aTZ	Varshni	НО	34.2	38.0	58.9	77.1
	Varshni	mA-6 (planar)	27.0	31.4	53.4	74.6
	НО	НО	21.0	29.4	52.6	74.6
CCSD(T)/aTZ	Varshni	НО	8.8	14.4	4.2	19.3
	Varshni	mA-6 (planar)	2.3	8.3	-0.7	18.5

does the further replacement of the harmonic triatomic potential with the planar mA-6 potential.

VI. CONCLUSIONS

The potential energy surfaces of polyatomic molecules are dominated by the effect of covalent bonding. This means that in the method we propose for constructing anharmonic potential energy surfaces from a sum of bonding potentials and triatomic potentials, the selection of the bonding potentials has the largest impact on the accuracy of the potential energy surfaces. However, we also demonstrate that the use of anharmonic triatomic potentials, which vanish with the dissociation of either one or both of the bonds, further improves the accuracy of potential energy surfaces and offers better agreement with vibrational spectroscopy data. In particular, we recommend the mA-3 triatomic potential for linear XY_2 -type molecules and the planar mA-5 potential for bent XY_2 -type molecules.

Extension of the methods evaluated here to further regions of chemical space introduces some additional challenges, such as the need to estimate the contributions of each bond to the total atomization energy; however, the possibility of reasonably accurate estimates of higher-order derivatives at a negligible computational cost could make the consideration of such further approximations justifiable. Future work will focus on extending the method outlined in Sec. I A to more complex geometries, such as XY_3 and XY_4 , using the approximation in Eq. (2) and also more generally to polyatomic molecules with multiple centers using bond dissociation energy estimating methods.

ACKNOWLEDGMENTS

This work was supported, in part, by the University of Pittsburgh Center for Research Computing through the resources provided. We specifically acknowledge the technical support of Barry Moore II and thank Hashim Yousif for constructive feedback.

AUTHOR DECLARATIONS

Conflict of Interest

The author has no conflicts to disclose.

Author Contributions

Daniel Sadowsky: Conceptualization (lead); Data curation (lead); Formal analysis (lead); Investigation (lead); Supervision (lead); Validation (lead); Visualization (lead); Writing – original draft (lead); Writing – review & editing (lead).

DATA AVAILABILITY

The data that support the findings of this study are available from the corresponding author upon reasonable request.

REFERENCES

- ¹S. Carter, S. J. Culik, and J. M. Bowman, "Vibrational self-consistent field method for many-mode systems: A new approach and application to the vibrations of CO adsorbed on Cu (100)," J. Chem. Phys. **107**, 10458–10469 (1997).
- ²J. M. Bowman, T. Carrington, and H.-D. Meyer, "Variational quantum approaches for computing vibrational energies of polyatomic molecules," Mol. Phys. **106**, 2145–2182 (2008).
- 3 M. Neff and G. Rauhut, "Toward large scale vibrational configuration interaction calculations," J. Chem. Phys. 131, 124129 (2009).
- ⁴M. Sibaev and D. L. Crittenden, "PyVCI: A flexible open-source code for calculating accurate molecular infrared spectra," Comput. Phys. Commun. **203**, 290–297 (2016)
- ⁵O. Christiansen, "Vibrational coupled cluster theory," J. Chem. Phys. 120, 2149–2159 (2004).
- ⁶P. Seidler, M. Sparta, and O. Christiansen, "Vibrational coupled cluster response theory: A general implementation," J. Chem. Phys. **134**, 054119 (2011).
- ⁷O. Christiansen, "Selected new developments in vibrational structure theory: Potential construction and vibrational wave function calculations," Phys. Chem. Chem. Phys. 14, 6672–6687 (2012).

- ⁸D. G. Truhlar, "A simple approximation for the vibrational partition function of a hindered internal rotation," J. Comput. Chem. **12**, 266–270 (1991).
- ⁹K. R. Glaesemann and L. E. Fried, "A path integral approach to molecular thermochemistry," J. Chem. Phys. 118, 1596–1603 (2003).
- ¹⁰D. Bakowies, "Estimating systematic error and uncertainty in *ab initio* thermochemistry: II. ATOMIC(hc) enthalpies of formation for a large set of hydrocarbons," J. Chem. Theory Comput. **16**, 399–426 (2019).
- ¹¹P. M. Morse, "Diatomic molecules according to the wave mechanics. II. Vibrational levels," Phys. Rev. 34, 57–64 (1929).
- ¹²I. Haslingerová, "Estimation of bond energies from Mulliken overlap populations," Czech. J. Phys. B 27, 1389–1393 (1977).
- ¹³X. Qu, D. A. Latino, and J. Aires-de-Sousa, "A big data approach to the ultra-fast prediction of DFT-calculated bond energies," J. Cheminf. 5, 34 (2013).
- ¹⁴K. Yao, J. E. Herr, S. N. Brown, and J. Parkhill, "Intrinsic bond energies from a bonds-in-molecules neural network," J. Phys. Chem. Lett. **8**, 2689–2694 (2017).
- ¹⁵H. Nakai, J. Seino, and K. Nakamura, "Bond energy density analysis combined with informatics technique," J. Phys. Chem. A 123, 7777–7784 (2019).
- ¹⁶M. Wen, S. M. Blau, E. W. C. Spotte-Smith, S. Dwaraknath, and K. A. Persson, "BonDNet: A graph neural network for the prediction of bond dissociation energies for charged molecules," Chem. Sci. 12, 1858–1868 (2021).
- ¹⁷S.-W. Chiu, H. L. Scott, and E. Jakobsson, "A coarse-grained model based on morse potential for water and n-alkanes," J. Chem. Theory Comput. 6, 851–863 (2010).
- ¹⁸K. Park, W. Lin, and F. Paesani, "A refined MS-EVB model for proton transport in aqueous environments," J. Phys. Chem. B **116**, 343–352 (2012).
- ¹⁹ R. J. Shannon, B. Hornung, D. P. Tew, and D. R. Glowacki, "Anharmonic molecular mechanics: Ab initio based morse parametrizations for the popular MM3 force field," J. Phys. Chem. A 123, 2991–2999 (2019).
- ²⁰Y. P. Varshni, "Comparative study of potential energy functions for diatomic molecules," Rev. Mod. Phys. 29, 664–682 (1957).
- ²¹ A. T. Royappa, V. Suri, and J. R. McDonough, "Comparison of empirical closed-form functions for fitting diatomic interaction potentials of ground state first- and second-row diatomics," J. Mol. Struct. 787, 209–215 (2006).
- ²² A. B. Anderson, "Simple potential energy function for CO₂," J. Chem. Phys. **56**, 4228–4229 (1972).

- ²³ A. B. Anderson, "Theoretical approach to potential energy functions for linear AB₂ and ABC and bent AB₂ triatomic molecules," J. Chem. Phys. **57**, 4143–4152 (1972).
- ²⁴T. Shimanouchi, *Tables of Molecular Vibrational Frequencies. Consolidated Volume I* (National Bureau of Standards, Washington, DC, 1972).
- ²⁵T. Shimanouchi, "Tables of molecular vibrational frequencies. Consolidated volume II," J. Phys. Chem. Ref. Data 6, 993–1102 (1977).
- ²⁶J. Tennyson, P. F. Bernath, L. R. Brown, A. Campargue, A. G. Császár, L. Daumont, R. R. Gamache, J. T. Hodges, O. V. Naumenko, O. L. Polyansky et al., "IUPAC critical evaluation of the rotational-vibrational spectra of water vapor, Part III: Energy levels and transition wavenumbers for H₂¹⁶O," J. Quant. Spectrosc. Radiat. Transfer 117, 29–58 (2013).
- ²⁷R. Tóbiás, T. Furtenbacher, A. G. Császár, O. V. Naumenko, J. Tennyson, J.-M. Flaud, P. Kumar, and B. Poirier, "Critical evaluation of measured rotational-vibrational transitions of four sulphur isotopologues of S¹⁶O₂," J. Quant. Spectrosc. Radiat. Transfer 208, 152–163 (2018).
- ²⁸D. G. A. Smith, L. A. Burns, A. C. Simmonett, R. M. Parrish, M. C. Schieber, R. Galvelis, P. Kraus, H. Kruse, R. Di Remigio, A. Alenaizan *et al.*, "PSI4 1.4: Open-source software for high-throughput quantum chemistry," J. Chem. Phys. **152**, 184108 (2020).
- ²⁹T. H. Dunning, Jr., "Gaussian basis sets for use in correlated molecular calculations. I. The atoms boron through neon and hydrogen," J. Chem. Phys. **90**, 1007–1023 (1989).
- ³⁰D. E. Woon and T. H. Dunning, Jr., "Gaussian basis sets for use in correlated molecular calculations. III. The atoms aluminum through argon," J. Chem. Phys. 98, 1358–1371 (1993).
- ³¹R. A. Kendall, T. H. Dunning, Jr., and R. J. Harrison, "Electron affinities of the first-row atoms revisited. Systematic basis sets and wave functions," J. Chem. Phys. **96**, 6796–6806 (1992).
- ³² A. Meurer, C. P. Smith, M. Paprocki, O. Čertík, S. B. Kirpichev, M. Rocklin, A. Kumar, S. Ivanov, J. K. Moore, S. Singh *et al.*, "SymPy: Symbolic computing in python," PeerJ Comput. Sci. 3, e103 (2017).
- ³³M. Sibaev and D. L. Crittenden, "The PyPES library of high quality semi-global potential energy surfaces," J. Comput. Chem. 36, 2200 (2015).
- ³⁴See https://github.com/danielsadowsky/psi2vci for script.